Am J Physiol Lung Cell Mol Physiol 313: L1154–L1163, 2017.
First published September 14, 2017; doi:10.1152/ajplung.00009.2017.

RESEARCH ARTICLE | *Biomarkers in Lung Diseases: From Pathogenesis to Prediction to New Therapies*

Element-based prognostics of occupational pneumoconiosis using micro-proton-induced X-ray emission analysis

Xiaodong He,[1,2]* Hao Shen,[1]* Zidan Chen,[2]* Caicai Rong,[1] Minqin Ren,[3] Likun Hou,[2] Chunyan Wu,[2] Ling Mao,[2] Quan Lu,[4] and Bo Su[2]

[1]*Key Laboratory of Applied Ion Beam Physics, Institute of Modern Physics, Fudan University, Shanghai, China;* [2]*Department of Pneumoconiosis, Occupational Disease Clinical Research Centre, Department of Radiotherapy, Central Laboratory, Department of Pathology, Shanghai Pulmonary Hospital, Tongji University School of Medicine, Shanghai, China;* [3]*Center for Ion Beam Applications, Department of Physics, National University of Singapore, Singapore; and* [4]*Departments of Environmental Health, Genetics, and Complex Diseases, Harvard T. H. Chan School of Public Health, Boston, Massachusetts*

Submitted 23 January 2017; accepted in final form 11 September 2017

He X, Shen H, Chen Z, Rong C, Ren M, Hou L, Wu C, Mao L, Lu Q, Su B. Element-based prognostics of occupational pneumoconiosis using micro-proton-induced X-ray emission analysis. *Am J Physiol Lung Cell Mol Physiol* 313: L1154–L1163, 2017. First published September 14, 2017; doi:10.1152/ajplung.00009.2017.—Pneumoconiosis is an occupational disease accompanied by long-term lung impairment, for which prediction of prognosis is poorly understood because of the complexity of the inhaled particles. Micro-proton-induced X-ray emission (micro-PIXE) analysis, which is advantageous for high-sensitivity, two-dimensional element mapping of lung tissues, was used to investigate element-based predictive factors of prognosis in Chinese patients with welder's and coal miner's pneumoconiosis. Chest radiographs and lung function tests showed that most of the coal miners deteriorated, whereas symptoms in some welders were alleviated after 5 yr, as determined by comparing percent vital capacity (%VC) and forced expiratory volume in the 1st second over forced vital capacity (FEV1.0/FVC) to values taken at the initial diagnosis. Micro-PIXE analysis suggested that the most abundant particulates in welder's pneumoconiosis were Fe, Mn, and Ti (metallic oxide),which were accompanied by particulates containing Si, Al, and Ca (aluminum silicate) or only Si (SiO_2); the most abundant particulates in coal miner's pneumoconiosis were composed of C, Si, Al, K, and Ti, which were accompanied by particulates containing Ca or Fe. Particulates containing Al, Si, S, K, Ca, and Ti (orthoclase and anorthite) were correlated with severity of fibrosis. Multivariable linear regression suggested that long-term FEV1.0/FVC decrease was independently associated with Si and smoking index, whereas %VC decrease was associated with Si and Ti. A risk index comprised of these factors was developed to predict the prognosis of pneumoconiosis. Micro-PIXE analysis is feasible for the evaluation of elemental composition and dust exposure, especially for patients whose exposure is mixed or uncertain.

micro-proton-induced X-ray emission analysis; pneumoconiosis; elemental analysis; lung function; lung biopsy

INTRODUCTION

Pneumoconiosis is a lung disease caused by the accumulation of inhaled inorganic dust and subsequent lung inflammation or fibrosis due to inadequate workplace protection. The dust may consist of a variety of minerals such as silica, aluminosilicate, and insoluble mixtures of metallic compounds (4, 5, 30). Occupational and environmental lung diseases still remain major causes of pulmonary impairment worldwide. According to the World Health Organization, pneumoconioses resulted in an estimated 30,000 deaths and almost 1.2 million disability-adjusted life years attributable to occupational airborne particulates globally (11). In China, more than 110,000 pneumoconiosis cases were newly diagnosed from 2007 to 2012 in patients whose occupations included coal worker, welder, founder, etc. New cases per year increased from 10,963 cases in 2007 to 26,873 cases in 2014 (31) (7).

Occupational history, chest radiographs, and pathological examinations are critical for the diagnosis of pneumoconiosis. The chemophysiological properties of inhaled particulates can result in varying inflammatory responses and fibrogenic activities, leading to different prognoses. At least 12 kinds of occupational pneumoconiosis have been legally described by the Ministry of Health of China. For example, silica (20) and asbestos (17) can cause progressive massive fibrosis, leading to lung function impairment and death. Respirable silica and silicates (10) were associated with rapidly progressive pneumoconiosis in U.S. coal workers. Beryllium is also reported to result in poor prognosis (13).

Unfortunately, obtaining accurate occupational history is sometimes difficult due to job changes, mixed exposures, or problems with poor reporting or recordkeeping. Moreover, routine pathological examinations for pneumoconiosis such as histology, polarizing microscopic observation of mineral crystal, and iron staining of biopsy tissue sections provide rather limited information about the chemical features of the inhaled dust (19). Precise determination of chemical features will benefit both diagnosis and prognostic prediction.

Micro-proton-induced X-ray emission (micro-PIXE) analysis has reportedly been used in the examination of elemental

* X. He, H. Shen, and Z. Chen contributed equally to this work.
Address for reprint requests and other correspondence: B. Su, Central Laboratory, Shanghai Pulmonary Hospital, Tongji Univ. School of Medicine, No. 507, Zhengmin Rd., Yangpu District, Shanghai, China (e-mail: su_bo_s@hotmail.com).

behavior in complicated structures such as human tissue sections (25) and provides elemental composition and trace concentrations for most elements ($Z \geq 12$) with high sensitivity (~ppm). It can also provide two-dimensional (2-D) elemental mapping, which is suitable for discriminating the elemental composition of particulates deposited in lung tissue sections. In this study, we evaluated the prognosis of typical welders' and coal miners' pneumoconiosis by chest radiographs and lung function tests over 5 year of follow-up care and determined the exact chemical element composition and localization of inhaled dust in lung tissue sections using micro-PIXE analysis and Rutherford backscattering spectrometry. The relationship between particulates' elemental compositions and patient prognosis was investigated.

MATERIALS AND METHODS

Study population and procedures. The patients in this study were drawn from the archives of pneumoconiosis diagnoses in Shanghai Pulmonary Hospital. Of the 184 welders and 66 coal miners who were newly diagnosed with pneumoconiosis from 2004 to 2010, only 45 welders and 14 coal miners met all of the following criteria: *1*) digital radiographic images of the chest available for the time of diagnosis and 5-yr follow-up; *2*) underwent transbronchoscopic lung biopsy (TBLB) and had at least two TBLB samples (from anterior and lateral basal segments of the right lower lobe) available; and *3*) had complete lung function test follow-up records for ≥5 yr. To investigate the precise contribution of inhaled particles, patients with any complications of chronic obstructive pulmonary disease (COPD), tuberculosis, asthma, or cardiopulmonary dysfunction in their anamneses were excluded; this left 25 welders (11 with COPD, 5 with tuberculosis, 2 with asthma, and 1 with cardiopulmonary dysfunction were excluded) and six coal miners (4 with COPD, 3 with tuberculosis, and 1 with asthma were excluded). All six coal miners were enrolled in the study, and six welders were selected by matched case control sampling, with sex (male vs. male) and age (45.0 ± 3.5 vs. 47.0 ± 4.6, $P = 0.42$) as matching variables. This study was approved by the Ethics Committee of Shanghai Pulmonary Hospital. Written, informed consent was obtained from all participants.

Chest radiograph, lung function measurement, and follow-up. The enrolled patients were subjected to digital X-ray chest imaging and lung function tests every 1 to 2 yr. Chest radiographs were reviewed independently by three qualified experts and categorized using the International Labour Organization (ILO) International Classification of Radiographs of Pneumoconioses, Revised Edition (2011) (15). Parenchymal abnormalities included both small opacities (round: p, q, r; irregular: s, t, u) and large opacities. Profusion was classified into one of four ordered categories and 12 subcategories by comparison with standard radiographs. The overall profusion of small opacities was determined according to 12-point ILO profusion scores by considering profusion as a whole over affected zones of the lungs.

Lung function tests were performed using a spirometer (Masterscreen-PFT; Jaeger, Hoechberg, Germany). A minimum of three satisfactory forced expiratory maneuvers were undertaken for each patient. Percent vital capacity (%VC), forced expiratory volume in the 1st second/forced vital capacity (FEV1.0/FVC), and percent diffusing capacity of the lungs for carbon monoxide ($\%DL_{CO}$) were measured.

Hematoxylin and eosin staining, iron staining, and grading of pulmonary fibrosis. Three serial 6-μm sections were cut from the paraffin-embedded lung tissue blocks. One section was used for hematoxylin and eosin staining and one for iron staining. The third section was adhered to mylar film by heating at 60°C for half an hour; the wax was washed three times with xylene and then subjected to micro-PIXE analysis. hematoxylin and eosin staining and Perls' Prussian blue staining for iron were performed according to a published protocol (26), and the sections were observed under an Olympus BX51 microscope with polarized accessories.

The severity of pulmonary fibrosis for biopsy sections was graded on a scale of zero to eight according to the previously published grading system by Ashcroft et al. (1). A greater score indicates more severe fibrosis. The grading for each sample was determined separately by two pathologists and arbitrated by a third senior pathologist, and the score for each patient was the rounded average of two or three tissue blocks.

Micro-PIXE analysis. Elemental analysis was performed at the National University of Singapore Research Centre for Nuclear Microscopy (24) using a 2.1-MeV proton beam from a 3.5-MeV high-brightness High Voltage Engineering Europa Singletron ion accelerator, which was focused to a 2-μm spot size. Three complementary ion beam techniques were simultaneously applied: *1*) micro-PIXE was used to measure the concentrations of elements such as Al, Si, and those above them in the periodic table, and a lithium-drifted silicon X-ray detector was placed at 45° to the beam axis and fitted with a 300-μm Perspex filter with a central hole of 1 mm in diameter; *2*) Rutherford backscattering spectrometry (RBS) provided information on matrix composition and incident charge, was used to extract quantitative results in conjunction with PIXE, and was also used to determine the 2-D distribution of carbon; *3*) off-axis scanning transmission ion microscopy (STIM) provided information on the structure and density distribution of the sample and facilitated positioning of the unstained sections before analysis. Three TBLB samples of idiopathic pulmonary fibrosis with no smoking history were used as the control group for baseline measurements, as a diagnosis of idiopathic pulmonary fibrosis excludes environmental dust or drugs as causes.

Statistical analysis. Statistical analyses were performed with SPSS 17.0 software (SPSS, Chicago, IL). Statistical differences in element concentrations between the two groups were calculated using the nonparametric Wilcoxon Mann-Whitney *U*-test. Pearson's or Spearman's correlation was used to evaluate the correlation coefficient of the two groups for continuous or discrete variables, respectively. Multivariate linear regression was used to model the effects of elements on the prognosis of the patients. The level of significance was defined as a P value of <0.05.

RESULTS

Demographic information and occupational history of the patients with pneumoconiosis. All of the 12 patients with pneumoconiosis were male, ranging from 39 to 54 yr old. According to their occupational history, six patients had had long-term exposure to welding dust while working as welders. *Patient no. 2* and *patient no. 3* utilized mainly manual arc welding, whereas the others utilized carbon dioxide-shielded welding. The average exposure duration was 17.2 ± 7.1 yr. The other six patients were diagnosed with coal miner's pneumoconiosis and had been exposed to coal dust in coal mines for 14.8 ± 5.2 yr on average. All patients had a history of smoking before diagnosis; five quit smoking completely during treatment, and the others smoked less or occasionally. Detailed occupational histories and smoking indexes for all patients are listed in Table 1.

Chest radiograph and lung function parameters of patients with pneumoconiosis over 5-yr follow-up. Chest radiographs are commonly used to evaluate the progression of pneumoconiosis. Radiographic findings from these 12 patients at the initial diagnosis and at 5-yr follow-up are shown in Table 2. None of the patients had large opacities, although three of the six coal miners had aggregation of small opacities at the initial diagnosis. After 5 yr, affected zones decreased in three of the six welder patients, and overall profusion decreased in two cases according to the 12-point ILO profusion scores. In

Table 1. *Occupational history of patients with pneumoconiosis*

Type of Pneumoconiosis	Sex	Age, yr	Occupational Exposure	Smoking Index*	Date of Diagnosis
Welder's pneumoconiosis					
Patient no. 1	Male	39	1990–2004: Arc-welding plant in shipyard	200	2004
Patient no. 2	Male	43	1984–2004: Welder	200	2005
Patient no. 3	Male	48	1985–1996: Arc-welding plant for pressure vessels; 1996–2008: welding plant for reefer containers.	350	2009
Patient no. 4	Male	45	1995–2010: Welder	400	2010
Patient no. 5	Male	48	1997–1999: Stoker, coal shoveling; 2001–2010: welder	300	2010
Patient no. 6	Male	47	1994–2010: Welder in boiler plant	100	2010
Coal worker's pneumoconiosis					
Patient no. 7	Male	48	1996–2004: Coal digger	360	2005
Patient no. 8	Male	45	1995–2006: Coal digger	310	2007
Patient no. 9	Male	50	2001–2008: Coal digger; 2009–2010: manual feeding of powder for lithium battery	800	2010
Patient no. 10	Male	54	1986–2004: Coal digger	450	2005
Patient no. 11	Male	44	1990–2001: Coal digger; 2001–2007: coal hauler	290	2007
Patient no. 12	Male	41	1998–2009: Underground coal hauler; April–September 2010: paint spraying worker	390	2010

*Cigarette years.

contrast, affected zones increased in five of six coal miner patients, of which overall profusion increased in three cases. Radiographs for representative patients with stable or changed profusion scores are presented in Fig. 1*A*. Changes in radiograph findings were limited, with only one subcategory ascending or descending after 5 yr.

Progressive impairment of lung function is a key feature in the prognosis of patients with pneumoconiosis (6), especially for silicosis (14). We also examined lung function parameters (LFPs) for all patients at the 5-yr follow-up. Ratios of LFPs in the 5th yr to values from the initial diagnoses were used to assess the progressive impairment of lung function. The ratios of %VC, FEV1.0/FVC, and $\%DL_{CO}$ did not decrease significantly in the welder's pneumoconiosis, but the ratios of %VC and FEV1.0/FVC did decrease significantly in the coal miner's pneumoconiosis (Fig. 1*B*). The ratios of %VC and FEV1.0/FVC are significantly correlated to variation in the ILO overall profusion score (%VC: Spearman $\rho = -0.635$, $P = 0.027$; FEV1.0/FVC: Spearman $\rho = -0.741$, $P = 0.006$). For deteriorated but not alleviated cases, radiographs showed visible signs corresponding to decreased %VC and FEV1.0/FVC(Fig. 1*C*). Compared with the graded ILO subcategories of chest radiographs, LFPs (%VC and FEV1.0/FVC) are subtle and more apt to reflect aggravation of the pneumoconiosis. The differences in prognosis between welders and coal miners suggest that the type of inhaled dust may result in divergent progression of the disease.

Pathologic examination and micro-PIXE analysis for patients exposed to welding dust. Lung samples for all six welder patients were positive for iron staining upon regular pathological examination, and three of them were also positive under polarizing microscopy (Fig. 2*A*). To explore the characteristics of inhaled particulates in the lung biopsy samples, we performed PIXE analysis on the sections. In contrast to conven-

Table 2. *ILO classification of chest radiographs for the patients with pneumoconiosis in the 5-yr follow-up*

	Predominant Small Opacity Shape/Size		Affected Zones		Overall Profusion of Small Opacities	
Type of Pneumoconiosis	A	B	A	B	A	B
Welder						
Patient no. 1	s/p	s/p	6	4	1/2	1/1*
Patient no. 2	p/q	p/q	5	5	2/1	2/1
Patient no. 3	p/s	p/s	4	4	1/2	1/1*
Patient no. 4	p/p	p/p	6	5	1/2	1/2
Patient no. 5	p/p	p/p	4	4	1/1	1/1
Patient no. 6	p/p	p/p	4	3	1/0	1/0
Coal worker						
Patient no. 7	q/p	q/p	5	5	2/1	2/1
Patient no. 8	p/q	p/q	5	6	2/1	2/2*
Patient no. 9	p/q	p/q	5	6	3/2	3/3*
Patient no. 10	p/p	p/p	5	6	3/2	3/3*
Patient no. 11	p/p	p/p	5	6	2/1	2/1
Patient no. 12	p/s	p/s	5	6	3/2	3/2

ILO, International Labour Organization. A, at the time of initial diagnosis; B, at the time after 5-yr follow-up. Small, rounded opacities are as follows: p, ≤1.5 mm; q, >1.5 and ≤3 mm; r, >3 and ≤10 mm. Large opacity: the longest dimension >10 mm; all patients were without large opacities. *Changed score.

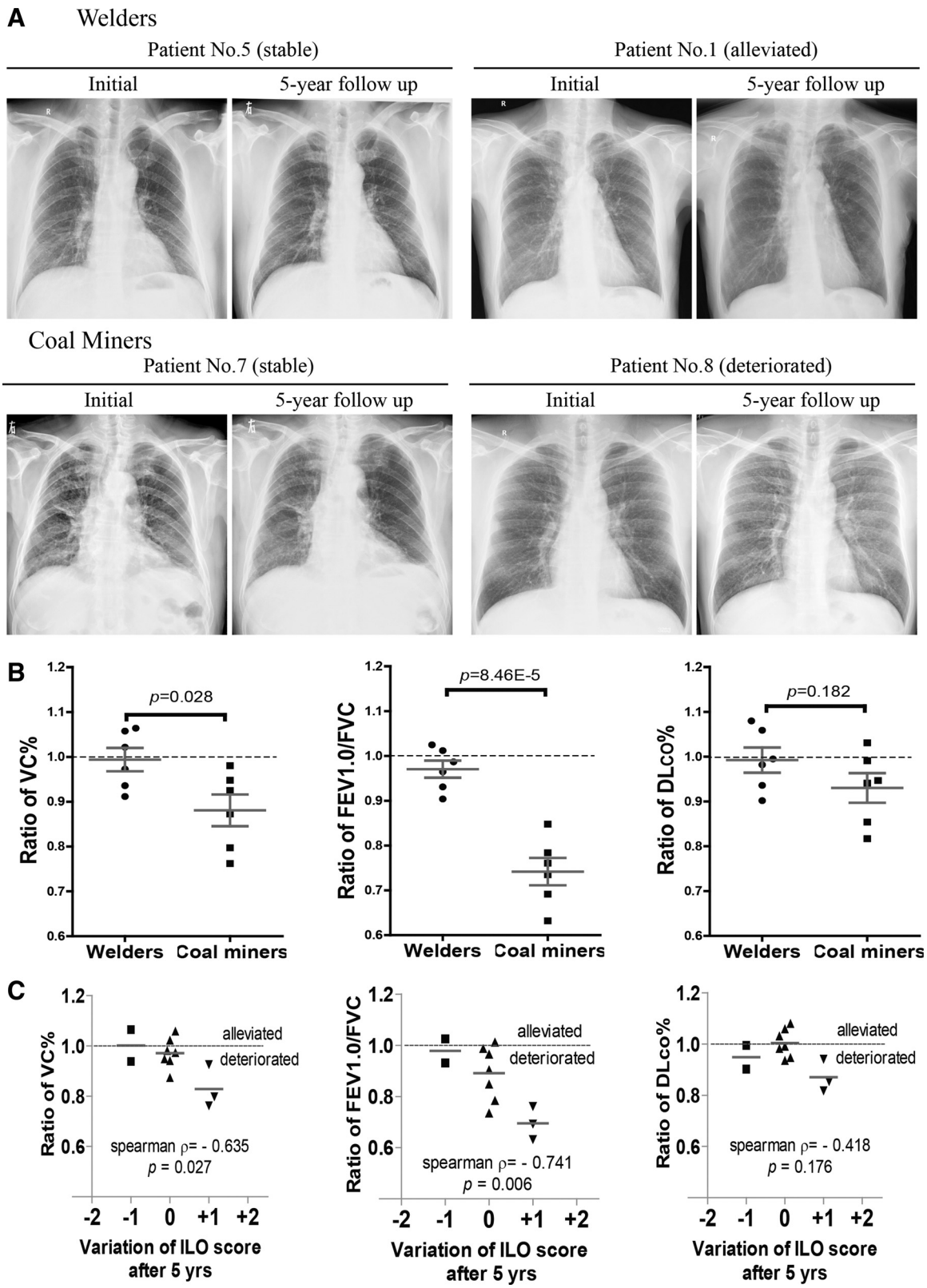

Fig. 1. Variation in chest radiograph and lung function parameters at 5-yr follow-up for patients with welder's or coal miner's pneumoconiosis. *A*: representative chest radiographs from the initial diagnosis and after 5-yr follow-up. Examples for stable and changed profusion scores are shown. *B*: ratios of lung function parameters [percent vital capacity (%VC), forced vital capacity (FEV1.0/FVC), and percent diffusing capacity of the lungs for carbon monoxide ($\%DL_{CO}$)] in the 5th yr of follow-up to values from the initial diagnosis. *C*: variation in International Labour Organization (ILO) profusion scores and the changed ratios of lung function parameters at the 5-yr follow-up. The *x*-axis represents variation in the 12-point ILO overall profusion score; the *y*-axis represents the ratio of lung function parameters in the 5th yr of follow-up to that at the initial diagnosis.

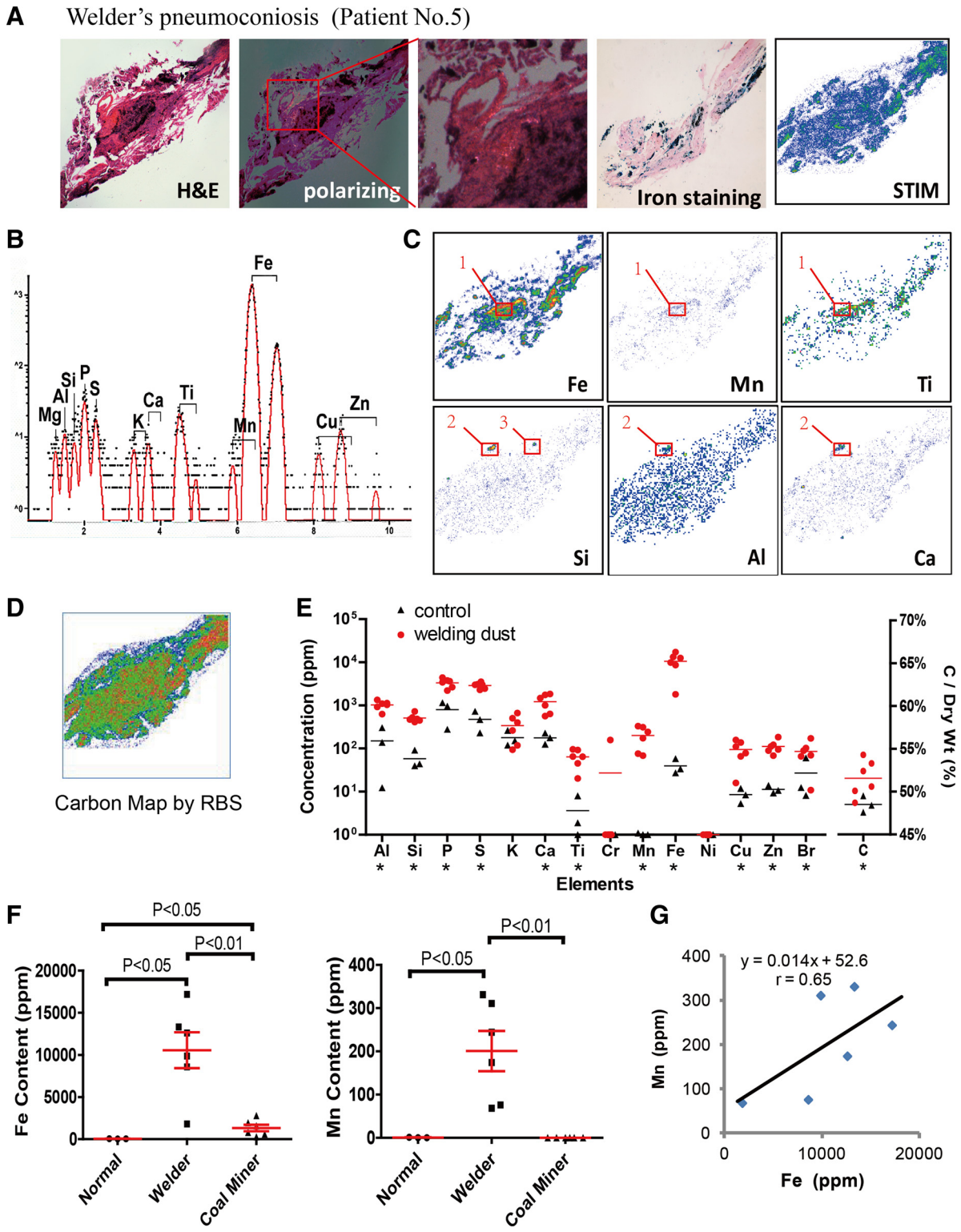

Fig. 2. Proton-induced X-ray emission (PIXE) analysis of patients exposed to welding dust. *A*: representative hematoxylin and eosin (H&E) staining, polarizing imaging, iron staining, and scanning transmission ion microscopy (STIM) of welder's pneumoconiosis (*patient no. 5*). *B*: PIXE spectrum for *patient no. 5*. *C*: elemental mapping suggesting the different particles deposited in the lung: "1" indicates particulates containing Fe, Mn, and Ti; "2" indicates particulates containing Si, Al, and Ca; "3" indicates particulates containing only Si. *D*: carbon mapping by Rutherford backscattering spectrometry of the lung section for *patient no. 5*. *E*: comparison of deposited element content in welder's pneumoconiosis with the control group (Mann-Whitney *U*-test, $*P < 0.05$). *F*: extreme elevation of Fe and Mn in welder's pneumoconiosis (Mann-Whitney *U*-test). *G*: the linear relation of Mn to Fe in welder's pneumoconiosis (Pearson's correlation, $r = 0.65$).

tional pathological examination, PIXE analysis provided more information on elemental content and distribution in the sections (Fig. 2, *B* and *C*). The carbon element for each section was determined by RBS and indicated as the carbon content per dry weight (%). With 2-D elemental mapping (Fig. 2, *C* and *D*), the colocalization of elements suggests the composition of the particular inhaled particulates. At least three kinds of particulates could be discriminated in the tissue. The most abundant particulates were composed of Fe, Mn, and Ti (metallic oxides). These are major components in welding fumes (18), and our results indicate that this kind of particulate is predominant in patients with welder's pneumoconiosis. The other two kinds of particulates, composed of Si, Al, and Ca (aluminum silicate) or only Si (SiO_2), were much less abundant.

Overall, Fe, Al, Si, Mn, Ti, Cu, Zn, Br, P, S, and C element contents were significantly increased in welder's pneumoconiosis compared with the control group, demonstrating the complex elemental composition of inhaled welding dust (Fig. 2*E*). Interestingly, Mn was found to be uniquely higher in all patients with welder's pneumoconiosis but undetectable in coal miner's pneumoconiosis (Fig. 2*F*). Meanwhile, Mn colocalized with Fe and presented a positive linear correlation with the amount of Fe in the patients with welder's pneumoconiosis (Fig. 2, *C* and *G*).

Pathological examination and micro-PIXE analysis of patients exposed to coal dust. Lung samples of all six patients with coal miner's pneumoconiosis were subjected to pathological examination and PIXE analysis. Five of the six patients were positive by the polarizing microscopy test, and two of the six were positive for iron staining (Fig. 3*A*). From 2-D elemental mapping, we identified the most abundant particulates in coal miner's pneumoconiosis as composed of Si, Al, K, and Ti, and the other two identified particulates contained Si, Al, and Ca or only Fe (Fig. 3, *B* and *C*). We proposed that the inhaled particles were mainly from orthoclase ($KAlSi_3O_8$) and anorthite ($CaAl_2Si_2O_8$), which are the two main ingredients of rock dust in the coal mines of China. The elements Al, Si, C, S, K, Ca, Ti, Fe, Cu, and Zn were found to be significantly increased in coal miner's pneumoconiosis compared with the control group, suggesting complexity in the composition of inhaled coal dust (Fig. 3*D*). Carbon dust usually accumulates greatly in the lungs of patients with coal miner's pneumoconiosis. Our results suggested that carbon was much higher in coal miner's pneumoconiosis than the normal or welder's pneumoconiosis samples and was colocalized with Si, Al, Fe, and Ti (Fig. 3*E*). In addition to carbon, the Si, Al, and Ti contents were especially higher in coal miners compared with welders (Fig. 3*G*). Si and Al were highly correlated ($r = 0.86$), indicating that aluminum silicate is another prevalent particulate deposited in the lungs of coal miners (Fig. 3*F*).

Correlation of inhaled elements and smoking index with severity of fibrosis at the initial diagnosis. The severity of fibrosis for each lung biopsy was graded on a scale of zero to eight. Of the six welders, five were Grade 3 and only one was Grade 5. Of the six coal miners, one was Grade 3, two were Grade 4, two were Grade 5, and one was Grade 6. The concentrations of Al, Si, S, K, Ca, and Ti correlated with the severity of fibrosis (Fig. 4*A*) with a coefficient of >0.6 ($P < 0.05$). C content was marginally correlated with fibrosis ($r = 0.549$, $P = 0.065$), and smoking index was not correlated with fibrosis in this cohort ($r = 0.114$, $P = 0.724$).

Radar charts of representative elements for each patient can objectively discriminate exposure history. PIXE analysis provides an objective and full-scale elemental composition of the inhaled dust, and we can establish a radar chart of elements for each patient with pneumoconiosis. Using these radar charts, we determined that the dust inhaled by coal miners is composed predominantly of C, Si, Al, and Ti, whereas that inhaled by welders is composed mainly of Fe and Mn (Fig. 4*B*). The radar chart provides objective evidence of inhaled dust composition, which gives quantitative exposure information to clinical physicians; this is especially important for patients whose occupational exposures are uncertain or mixed.

Development of an inhaled chemical element-based risk index to predict prognosis of pneumoconiosis. FEV1.0/FVC and %VC are sensitive indexes that reflect airway obstruction and fibrosis defects in patients with pneumoconiosis (22). To evaluate which elements relate to the decreased FEV1.0/FVC and %VC values, multivariable linear regression was performed, using the inhaled element contents and smoking index as variables. As shown in Table 3, Si content and smoking index were independently associated with the decrease of FEV1.0/FVC, whereas Si and Ti were independent factors for the decrease of %VC. These results suggest that Si and the smoking index contributed to the long-term decrease of FEV1.0/FVC, whereas Si and Ti contribute to the long-term decrease in %VC.

Inhaled particulates have different associations with airway inflammatory obstruction and pulmonary fibrosis because of their different chemophysiological characteristics. Utilizing the above multivariable linear regression, we established an element-based model to predict the prognosis of pneumoconiosis, i.e., risk index = 1.200E-4 × Si + 2.969E-4 × Ti + 4.142E-4 × (smoking index). Coefficients were taken from the averages of variable coefficients in the linear regression equations for both FEV1.0/FVC and %VC, and the equation was normalized to the 0 to 1 range. This risk index comprised of Si, Ti, and smoking index can predict the FEV1.0/FVC decrease of patients with pneumoconiosis ($r^2 = 0.86$) as well as the decrease in %VC ($r^2 = 0.80$) and $\%DL_{CO}$ ($r^2 = 0.59$) (Fig. 5).

DISCUSSION

In China, the annual rate of occupational health surveillance covers only ~30% of workers exposed to dust. Aside from silicosis, coal miner's pneumoconiosis and welder's pneumoconiosis are the most prevalent occupational diseases in China. It is known that inhaled silica dust (SiO_2) is the cause of silicosis, but the inhaled dust involved in coal miner's pneumoconiosis and welder's pneumoconiosis is much more complicated.

Legal pneumoconiosis is identified by occupation and inhaled dust, which is not suggestive of pathological and clinical characteristics (12). Dust-induced airway inflammatory obstruction and pulmonary fibrosis are the two major progressive symptoms for pneumoconiosis. In the view of physicians, pneumoconiosis may be clinicopathologically classified as either fibrotic or nonfibrotic. Sustained pulmonary fibrosis caused by fibrogenic inhaled dust can lead to progressive lung function impairment and eventually death for patients with pneumoconiosis (8).

The elemental composition of inhaled dust has varied ability to lead to airway inflammation and pulmonary fibrosis (2).

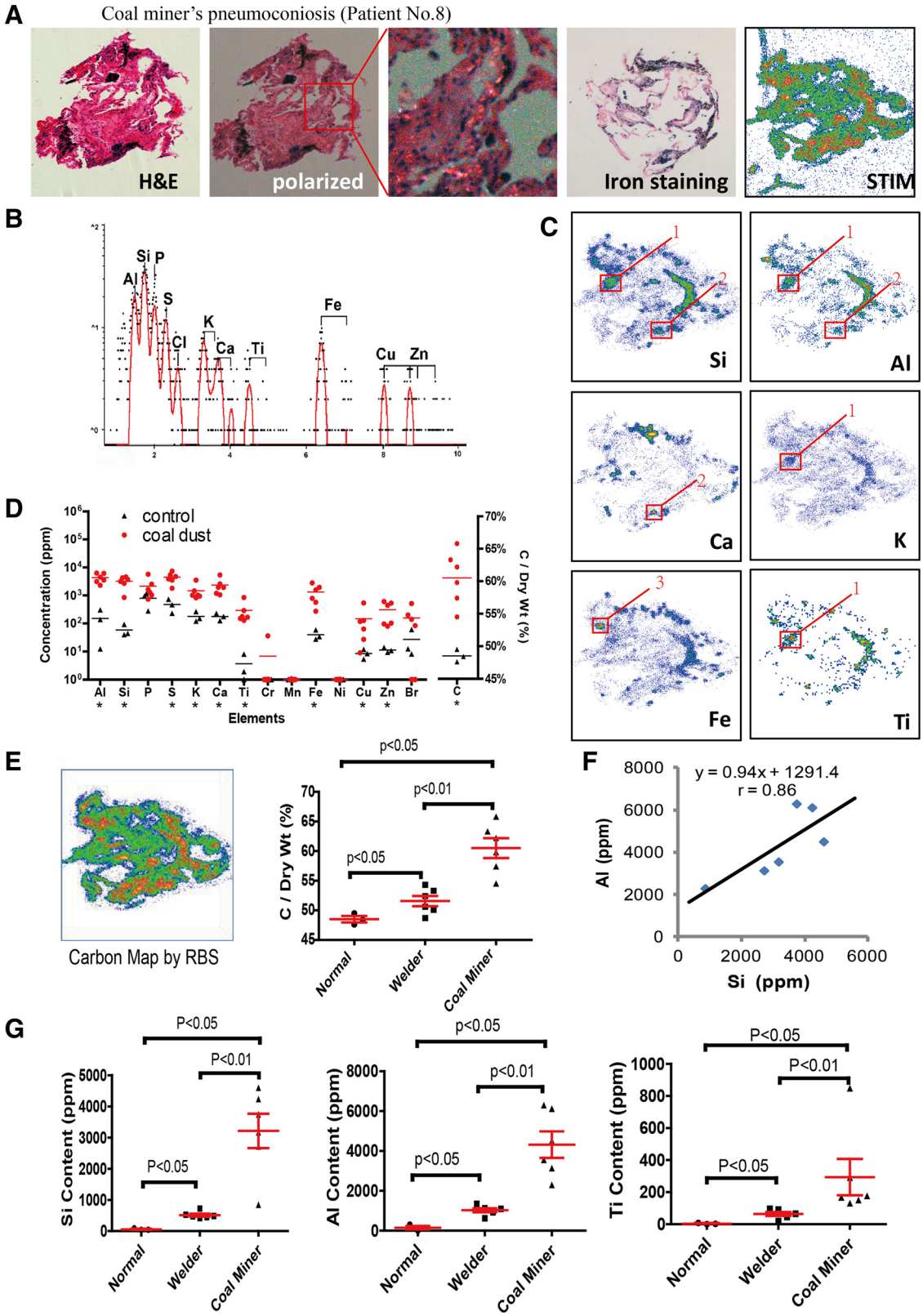

Fig. 3. Proton-induced X-ray emission (PIXE) analysis of patients exposed to coal dust. *A*: representative PIXE analysis. Light microscopy (H&E staining, polarized light, and iron staining) and scanning transmission ion microscopy (STIM) of coal miner's pneumoconiosis (*patient no. 8*). *B*: PIXE spectrum for *patient no. 8*. *C*: elemental mapping suggesting the different particles deposited in the lung: "1" indicates particulates containing Si, Al, K, and Ti; "2" indicates particulates containing Si, Al, and Ca; "3" indicates particulates containing Fe. *D*: comparison of deposited element content in coal miner's pneumoconiosis with the control group. *E*: carbon mapping by Rutherford backscattering spectrometry of the lung section for *patient no. 8* (*left*). Carbon content/dry weight (%) in lung samples of the controls, welders, and coal miners (*right*). *F*: the linear relation of Si to Al in coal miner's pneumoconiosis (Pearson's correlation, $r = 0.86$). *G*: significant elevation of Si, Al, and Ti only in coal miner's pneumoconiosis (Mann-Whitney *U*-test).

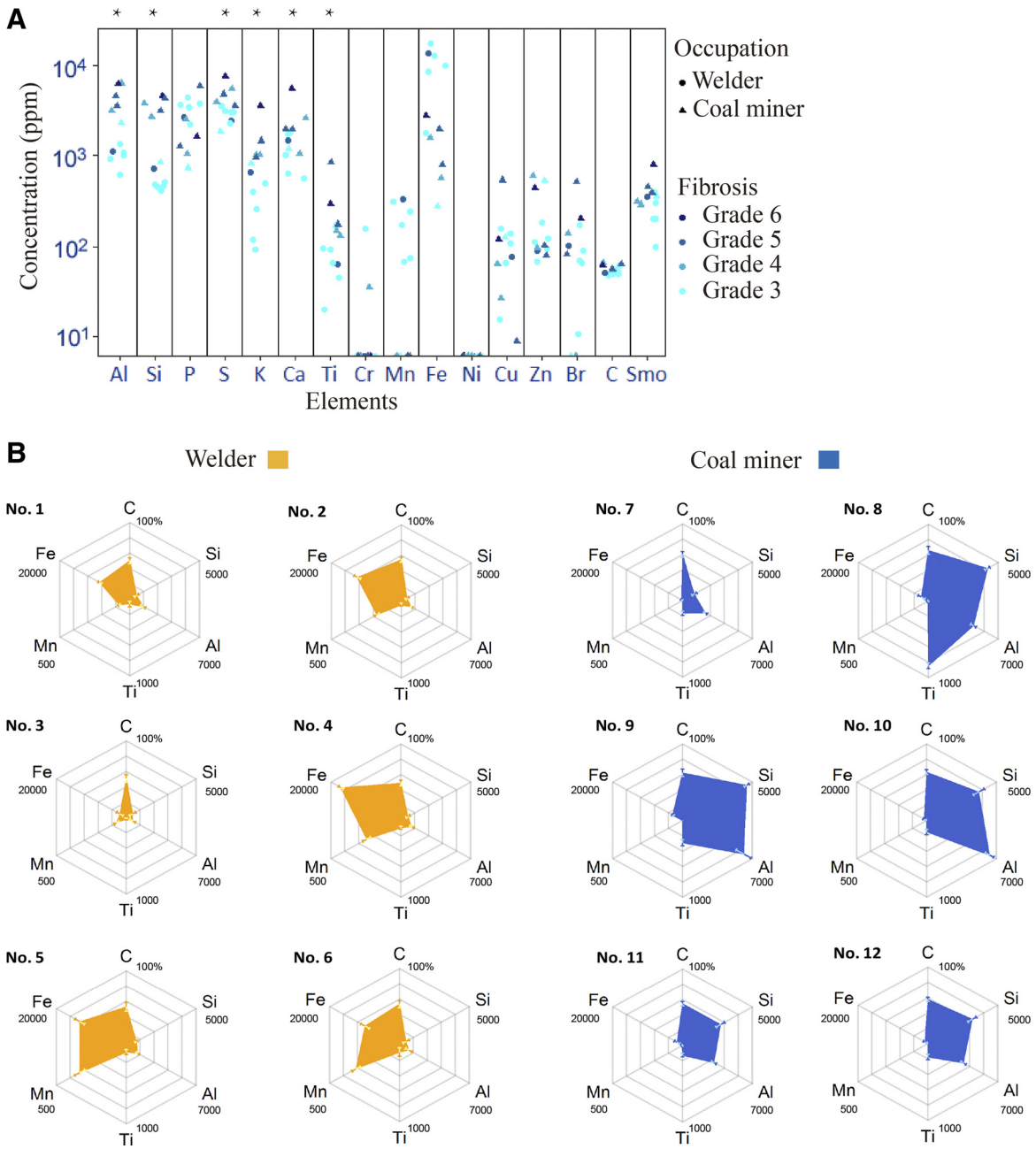

Fig. 4. *A*: correlation between fibrosis and inhaled elements in the biopsy sections at the time of initial diagnosis (*Spearman's correlation, $r > 0.6$, $P < 0.05$). Smo, smoking index. *B*: discrimination of exposure history between welders and coal miners by radar chart. Welders fell on the *left* side of the C-Ti axis and coal miners on the *right*. Error bars, range.

Elemental analysis of inhaled particulates by micro-PIXE makes it possible to investigate the association of inhaled elements with the prognosis of pneumoconiosis. Taking advantage of micro-PIXE and lung function tests, we evaluated the relationship of inhaled elements with the prognosis of pneumoconiosis patients and found that Si and smoking index were independently related to FEV1.0/FVC decrease, whereas Si and Ti were related to %VC decrease. Of note is that Si was identified as an independent risk factor for both FEV1.0/FVC and %VC decrease in this study, suggesting its important role in the progress of pneumoconiosis. Recently, Cohen et al. (10) determined that inhaled silica and silicates are responsible for rapidly progressive pneumoconiosis in U.S. coal workers, which is consistent with our result.

Additionally, we developed a risk index comprised of Si, Ti, and smoking status to predict the prognosis of pneumoconiosis in China, which may help to determine appropriate medical care. In this risk index, smoking is a well-established cause of airway inflammatory obstruction (9); silica and aluminosilicate particulates are considered to be fibrogenic factors based on both animal models and clinical evidence, and titanium dioxide can induce lung inflammation (21) and fibrosis (3) in animal models.

Table 3. *Association of inhaled chemical elements contents with the decrease of %VC and FEV1.0/FVC (in the 5th yr/at initial diagnosis) by multivariable linear regression*

FEV1.0/FVC			%VC		
Variables	coefficients	*P* value	Variables	Coefficients	*P* value
		Variables in model			
Constant	1.049	2.507E-10*	Constant	1.027	2.89E-12*
Si	−5.21E-05	0.002*	Si	−2.79E-05	0.036*
Smoking index	−2.76E-04	0.046*	Ti	−1.98E-04	0.045*
		Variables excluded			
			Smoking index	−0.347	0.089
P	0.130	0.315	P	0.157	0.513
S	0.425	0.056	S	−0.092	0.779
C	−0.353	0.090	C	0.022	0.941
Fe	0.178	0.268	Fe	−0.232	0.259
Mn	0.160	0.381	Mn	−0.308	0.137
Ti	−0.107	0.529			
Al	−0.292	0.464	Al	−0.089	0.879
Cu	−0.085	0.508	Cu	−0.099	0.570
Cl	−0.045	0.781	Cl	−0.102	0.678
K	0.265	0.394	K	−0.279	0.300
Ca	0.406	0.088	Ca	−0.155	0.528
Cr	0.152	0.236	Cr	0.237	0.140
Zn	−0.158	0.232	Zn	−0.065	0.734
Br	0.099	0.502	Br	0.239	0.477

%VC, %vital capacity; FEV1.0/FVC, forced expiratory volume in the 1st second over forced vital capacity. *$P < 0.05$.

Although pure coal dust has been confirmed to cause lung disorder, we identified at least two other kinds of deposited dust in the lung biopsies of coal miners in China using the 2-D elemental mapping capability of PIXE. We speculated that these two kinds of dust were crystalline silica, registering simply as Si, and aluminum silicates, including $KAlSi_3O_8$ (orthoclase) and $CaAl_2Si_2O_8$ (anorthite) from rock dust, detected as the combination of Si, Al, and K or Ca. It has been reported that coal dust in the mines in most provinces of China contains ~4–10% silica (27), and our data suggests that silica and aluminum silicate particulates cannot be neglected in the etiology and prognosis of coal miner's pneumoconiosis in China.

Two-dimensional elemental mapping of welder's pneumoconiosis suggests that deposited Fe and Mn were mostly concomitant in their lung samples, accompanied with sporadic silica. These particulates have been reported as the main components in welding fumes (16). Inhaled manganese is of greater concern because it can cause damage to the central nervous system, lungs, liver, and kidneys. Male workers exposed to manganese also have a higher risk of fertility problems. Prolonged exposure to manganese may cause Parkinson-like symptoms known as "manganism." Our results suggest that Mn deposition is as common as Fe in welder's pneumoconiosis, and greater attention should be given to this in its diagnosis and treatment. Notably, some welders may work in environments with silica dust contamination or be exposed to it from work in other occupations; this mixed inhaled silica dust can also be detected occasionally by micro-PIXE.

To illustrate the variety of dust exposures for single patients, we generated radar charts for each individual to indicate the inhaled elements and amounts, which can provide physicians with a visual and simple way to understand the exposure type and extent. In our study, welder's and coal miner's pneumoconiosis can be clearly discriminated by these radar charts. Currently, occupational exposure assessment in the diagnosis of pneumoconiosis depends mainly on occupational history certification, investigation of the occupation hygiene field, and self-reports. Sometimes, the reported dust exposures are subjective and one-sided, especially for the migrant workers, which account for a majority of the labor force in some Chinese areas. For those with uncertain or mixed exposures, micro-PIXE analysis or X-ray energy-dispersive spectrometry can provide objective and accurate assessment of exposures.

X-ray energy-dispersive spectrometry in scanning electron microscopes has been used for elemental analysis of biopsy samples. Micro-PIXE utilizes a proton microprobe instead of an electron microprobe to determine trace element composition and distribution. Because of the low bremsstrahlung background produced when high energy protons interact with a specimen, the sensitivity of micro-PIXE is nearly three orders of magnitude higher than that of electron-induced X-ray emission (23). Addi-

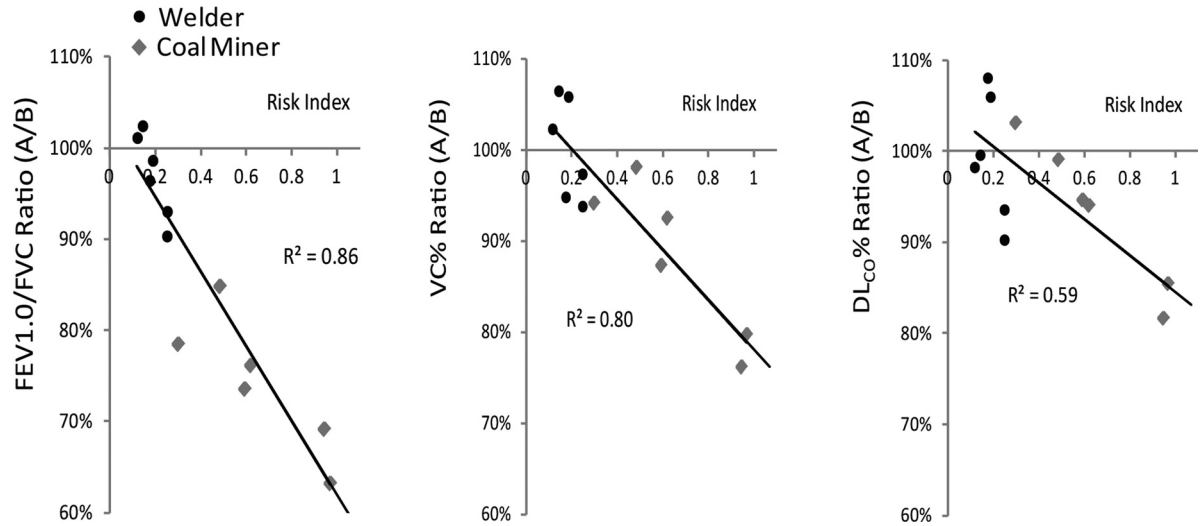

Fig. 5. The association between lung function impairment and risk index in patients with pneumoconiosis. *x*-Axis: risk index = 1.200E-4 × Si+2.969E-4 × Ti + 4.142E-4 × (smoking index); *y*-axis: the ratio of FEV1.0/FVC, %VC, or $\%DL_{CO}$ in the 5th yr of follow-up to values at the initial diagnosis.

tionally, the 3-MeV proton beam can penetrate a dozen micrometers beneath the surface of the specimen (29), whereas an electron beam can only penetrate to below 2 μm (28). Both elemental composition and the quantity of inhaled dust for each patient can be accurately determined by micro-PIXE.

Because of the complexity of inhaled particles, the long-term toxicity for inhaled dust is seldom evaluated precisely based on element composition. We evaluated chest radiographs and lung function (%VC, FEV1.0/FVC, and $\%DL_{CO}$) at the 5-yr follow-up for Chinese patients with welder's and coal miner's pneumoconiosis and developed an element-based risk index for prediction of prognosis. It should be noted that this risk index reflects only the contributions of particles to prognosis. Other factors such as medical complications should also be considered in clinical practice. Although the chemical element-based risk index in this study needs to be validated in in larger clinical samples, it provides an approach for evaluating the contribution of inhaled elements to prognosis and may benefit medical care for the patients with pneumoconiosis.

GRANTS

This work was funded by National Natural Science Foundation of China Grant 81572269, Science and Technology Commission of Shanghai Municipality Grants 14411966400, 134119a3400, and 15ZR1434500, and Shanghai Health Bureau Foundation Grants 201440397 and XYQ2013115.

DISCLOSURES

No conflicts of interest, financial or otherwise, are declared by the authors.

AUTHOR CONTRIBUTIONS

X.H., H.S., and B.S. conceived and designed research; X.H., H.S., Z.C., C.R., M.R., L.H., and B.S. performed experiments; X.H., H.S., Z.C., C.R., M.R., C.W., L.M., Q.L., and B.S. analyzed data; X.H., H.S., Z.C., M.R., L.H., C.W., L.M., and Q.L. interpreted results of experiments; X.H. drafted manuscript; X.H., H.S., Q.L., and B.S. edited and revised manuscript; H.S., Z.C., C.R., M.R., and L.H. prepared figures; B.S. approved final version of manuscript.

REFERENCES

1. **Ashcroft T, Simpson JM, Timbrell V.** Simple method of estimating severity of pulmonary fibrosis on a numerical scale. *J Clin Pathol* 41: 467–470, 1988. doi:10.1136/jcp.41.4.467.
2. **Bégin R, Cantin A, Massé S.** Recent advances in the pathogenesis and clinical assessment of mineral dust pneumoconioses: asbestosis, silicosis and coal pneumoconiosis. *Eur Respir J* 2: 988–1001, 1989.
3. **Bermudez E, Mangum JB, Wong BA, Asgharian B, Hext PM, Warheit DB, Everitt JI.** Pulmonary responses of mice, rats, and hamsters to subchronic inhalation of ultrafine titanium dioxide particles. *Toxicol Sci* 77: 347–357, 2004. doi:10.1093/toxsci/kfh019.
4. **Cao S, Duan X, Zhao X, Ma J, Dong T, Huang N, Sun C, He B, Wei F.** Health risks from the exposure of children to As, Se, Pb and other heavy metals near the largest coking plant in China. *Sci Total Environ* 472: 1001–1009, 2014. doi:10.1016/j.scitotenv.2013.11.124.
5. **Chen W, Liu Y, Wang H, Hnizdo E, Sun Y, Su L, Zhang X, Weng S, Bochmann F, Hearl FJ, Chen J, Wu T.** Long-term exposure to silica dust and risk of total and cause-specific mortality in Chinese workers: a cohort study. *PLoS Med* 9: e1001206, 2012. doi:10.1371/journal.pmed.1001206.
6. **Chia KS, Ng TP, Jeyaratnam J.** Small airways function of silica-exposed workers. *Am J Ind Med* 22: 155–162, 1992. doi:10.1002/ajim.4700220203.
7. **China National Health and Family Planning Commission.** Epidemic situation of reported occupational diseases of China in 2014 (Chinese). *Occup Health Emerg Rescue* 33: 1, 2015.
8. **Chong S, Lee KS, Chung MJ, Han J, Kwon OJ, Kim TS.** Pneumoconiosis: comparison of imaging and pathologic findings. *Radiographics* 26: 59–77, 2006. doi:10.1148/rg.261055070.
9. **Churg A, Tai H, Coulthard T, Wang R, Wright JL.** Cigarette smoke drives small airway remodeling by induction of growth factors in the airway wall. *Am J Respir Crit Care Med* 174: 1327–1334, 2006. doi:10.1164/rccm.200605-585OC.
10. **Cohen RA, Petsonk EL, Rose C, Young B, Regier M, Najmuddin A, Abraham JL, Churg A, Green FH.** Lung pathology in U.S. coal workers with rapidly progressive pneumoconiosis implicates silica and silicates. *Am J Respir Crit Care Med* 193: 673–680, 2016. doi:10.1164/rccm.201505-1014OC.
11. **Driscoll T, Nelson DI, Steenland K, Leigh J, Concha-Barrientos M, Fingerhut M, Prüss-Ustün A.** The global burden of non-malignant respiratory disease due to occupational airborne exposures. *Am J Ind Med* 48: 432–445, 2005. doi:10.1002/ajim.20210.
12. **Fraser R, Muller N, Colman N.** Inhalation of inorganic dust (pneumoconiosis). In: *Diagnosis of Diseases of the Chest (4th Ed.)*. Philadelphia, PA: Saunders, 1999, p. 99.
13. **Freiman DG, Hardy HL.** Beryllium disease. The relation of pulmonary pathology to clinical course and prognosis based on a study of 130 cases from the U.S. beryllium case registry. *Hum Pathol* 1: 25–44, 1970. doi:10.1016/S0046-8177(70)80003-X.
14. **Hnizdo E.** Loss of lung function associated with exposure to silica dust and with smoking and its relation to disability and mortality in South African gold miners. *Br J Ind Med* 49: 472–479, 1992.
15. **International Labour Office.** *Guidelines for the Use of the ILO International Classification of Radiographs of Pneumoconioses*. Geneva: International Labour Office, 2002.
16. **Li GJ, Zhang LL, Lu L, Wu P, Zheng W.** Occupational exposure to welding fume among welders: alterations of manganese, iron, zinc, copper, and lead in body fluids and the oxidative stress status. *J Occup Environ Med* 46: 241–248, 2004. doi:10.1097/01.jom.0000116900.49159.03.
17. **Markowitz SB, Morabia A, Lilis R, Miller A, Nicholson WJ, Levin S.** Clinical predictors of mortality from asbestosis in the North American Insulator Cohort, 1981 to 1991. *Am J Respir Crit Care Med* 156: 101–108, 1997. doi:10.1164/ajrccm.156.1.9610108.
18. **Matczak W, Przybylska-Stanisławska M.** [Determination of fumes and their elements from flux cored arc welding]. *Med Pr* 55: 481–489, 2004.
19. **McDonald JW, Roggli VL.** Detection of silica particles in lung tissue by polarizing light microscopy. *Arch Pathol Lab Med* 119: 242–246, 1995.
20. **Ng TP, Chan SL, Lee J.** Predictors of mortality in silicosis. *Respir Med* 86: 115–119, 1992. doi:10.1016/S0954-6111(06)80226-X.
21. **Park EJ, Yoon J, Choi K, Yi J, Park K.** Induction of chronic inflammation in mice treated with titanium dioxide nanoparticles by intratracheal instillation. *Toxicology* 260: 37–46, 2009. doi:10.1016/j.tox.2009.03.005.
22. **Prowse K, Allen MB, Bradbury SP.** Respiratory symptoms and pulmonary impairment in male and female subjects with pottery workers' silicosis. *Ann Occup Hyg* 33: 375–385, 1989.
23. **Ren CG, Zhou SJ, Che JM, Hu YD, Chen JX, Fang DF, Yang FJ.** A micromeam system of high energy ions at fudan university. *Nucl Sci Tech* 2: 6, 1991.
24. **Ren MQ, Thong PS, Makjanic J, Ponraj D, Watt F.** Nuclear microscopy in the life sciences at the National University of Singapore. A review. *Biol Trace Elem Res* 71-72: 65–76, 1999. doi:10.1007/BF02784192.
25. **Shimizu Y, Dobashi K.** Proton ion-microbeam elemental analysis for inhaled particle-induced pulmonary diseases: application for diagnosis and assessment of progression. *Curr Med Chem* 20: 789–793, 2013.
26. **Thompson AB, Bohling T, Heires A, Linder J, Rennard SI.** Lower respiratory tract iron burden is increased in association with cigarette smoking. *J Lab Clin Med* 117: 493–499, 1991.
27. **Wang ZQ, Wang PJ, Lian SQ.** Investigation on the content of free crystalline silica in coal dust from coal-mines in Gansu province of China. *Educ Occup Health* 23: 100–101, 2005.
28. **Watanabe K, Miyakawa O, Kobayashi M.** New method for quantitative mapping of metallic elements in tissue sections by electron probe microanalyser with wavelength dispersive spectrometers. *J Electron Microsc (Tokyo)* 50: 77–82, 2001. doi:10.1093/jmicro/50.1.77.
29. **Watt F.** The nuclear microprobe: a unique instrument. *Nucl Microprobe Tech Appl* 130: 8, 1997.
30. **Zhang M, Wang D, Zheng YD, Du XY, Chen SY.** [Analyses on the characteristics and the trends of pneumoconiosis notified between 1997 and 2009, in China]. *Zhonghua Lao Dong Wei Sheng Zhi Ye Bing Za Zhi* 31: 321–334, 2013.
31. **Zhang X, Ji JM, Zhang ZD.** Analysis on epidemiological characteristics and trends of occupational diseases in China from 2007 to 2012. *Occup Health (Chinese)* 32: 3, 2014.